AIMS Mathematics, 10(11): 26867–26883.
DOI: 10.3934/math.20251181
Received: 26 September 2025
Revised: 05 November 2025
Accepted: 14 November 2025
Published: 20 November 2025

https://www.aimspress.com/journal/Math

*Research article*

# Fault detection filter design for Markov jump systems with persistent dwell-time

**Zheng-Jin Zhang**[1,2] **and Bin-Bin Gan**[1,2,*]

[1] School of Automation, Qingdao University, Qingdao 266071, China
[2] Shandong Key Laboratory of Industrial Control Technology, Qingdao University, Qingdao 266071, China

* **Correspondence:** Email: gbbdyx@126.com.

**Abstract:** This paper addresses the problem of fault detection (FD) for Markov jump systems (MJSs) with time-varying delays. The jumping property presented by system modes is described by the Markov chain and the transition probabilities of the Markov chain are described by adopting the more flexible persistent dwell-time (PDT) switching rule. By introducing a filter to establish a residual system, the problem was converted into an $H_\infty$ filtering problem. The problem is complicated by the coexistence of time constraints in the PDT switching law and time-varying delays. By combining the Lyapunov-Krasovskii (L-K) method and switched system theory, a suitable filter was designed and a new PDT constraint was obtained. Ultimately, a virus mutation system model was used to demonstrate the practicability and effectiveness of the designed FD filter.

**Keywords:** Markov jump systems; fault detection filter; persistent dwell-time; time delays
**Mathematics Subject Classification:** 93D30, 93C55, 93B70

## 1. Introduction

Markov jump systems (MJSs) are stochastic systems that alternate among various operational modes, with the transitions being governed by a Markov process. For a long time, MJSs have strong modeling ability because of their unique advantage of using a Markov chain to accurately describe system changes [1]. In the last few years, MJSs have received more and more research interest and have been widely used in power system [2], network control systems [3–5], and so on.

With the increasing complexity of industrial system architectures, the need for system security increases [6, 7]. Some MJSs will inevitably encounter various faults in actual operation, like actuator faults, sensor faults, and so on. These faults not only affect the normal operation of the system, but also may cause major accidents. Therefore, how to find the faults timely has become an important

topic. Fault detection (FD) technology is designed to solve this problem, which can quickly and accurately identify potential failures [8, 9]. Based on the $H_\infty$ filter method, FD technology has been successfully applied in many kinds of MJSs, including, but not limited to, fuzzy semi-MJSs [10], conic-type MJSs [11], and positive MJSs [12]. However, existing FD filter designs largely presume simple switching patterns, whereas real-world MJSs exhibit more complex dynamics that intensify the impact of faults. This gap motivates the present work to devise a filter-based FD scheme, centered on a residual system synthesized from a filter and a fault weighting model, capable of accommodating such complexity.

Traditional MJSs with fixed transition probabilities often fail to accurately represent practical scenarios, where external disturbances and varying operational conditions cause these probabilities to change over time. To better characterize such real-world situations, researchers have adopted various switching rules to describe time-varying transition probabilities. Researchers have investigated MJSs governed by piecewise constant transition probabilities adhering to dwell-time switching rules [13]. Due to poor adaptability to high frequency switching, the dwell-time switching rule has been gradually replaced by other rules. The average dwell-time switching rule allows switching to take place in a short time interval. But the above two switching rules have the problem of limited switching frequency. The persistent dwell-time (PDT) switching rule works by introducing regions with fast and slow switching frequencies [14, 15]. It also allows free switching within the fast switching area. In contrast, the PDT switching rule is considered as a more general switching rule. The PDT switching rule determines the evolution of transition probabilities in MJSs, establishing a structured framework where the switching mechanisms govern the time-varying nature of stochastic transitions [16]. However, the FD for MJSs with PDT switching remains largely unexplored. This paper aims to fill this research gap by developing a novel FD filter specifically designed for such systems.

Due to limitations in response speed and transmission media, time delays may occur in MJSs [17, 18]. The time-delay phenomenon means that the current state is not only dependent on the current input, but is also inevitably affected by past inputs or states [19, 20]. This phenomenon will defer updating the switching signals, adding complexity to the system with the PDT switching rule [21]. Furthermore, time delays may result in delayed detection of fault signals or even mask the early fault signals. To solve the above problems, the Lyapunov-Krasovskii (L-K) functional method is usually used, which can consider both the boundary and the change of time delays. In order to employ more effective FD methods, using the L-K method to account for time delays and the PDT switching rule still has outstanding research potential. This is our third motivation for this study.

On this basis, the objective of this paper is to address the FD for a specific class of MJSs that incorporate time delays and PDT. The main contributions of this work are threefold:

(1) The time-varying transition probabilities of the continuous-time MJSs are characterized by the PDT switching rule, which offers greater flexibility and practical relevance compared to the dwell-time and average dwell-time rules used in prior studies.
(2) A novel FD filter design framework is established for MJSs subject to both PDT switching and time-varying delays, which effectively transforms the FD problem into an $H_\infty$ filtering problem.
(3) New stability and performance conditions are derived by integrating switched system theory with the L-K functional method, effectively handling the hybrid dynamics caused by time delays and PDT switching.

*Notations*: Throughout this article, $\mathbb{R}^n$ represents the $n$-dimensional vector space of the real number

field; $l_2[0,\infty)$ represents the set of squared integrable functions on $(0,\infty)$; $\mathrm{Sym}\{Q\} = Q + Q^T$; $*$ represents the symmetry element of a matrix; $Q > 0$ shows that $Q$ is positive definite; and $\mathrm{diag}\{\cdots\}$ means a diagonal matrix.

## 2. Problem formulation

This section outlines the problem and introduces a few preliminary concepts. The framework of FD filtering for MJSs with PDT is shown in Figure 1.

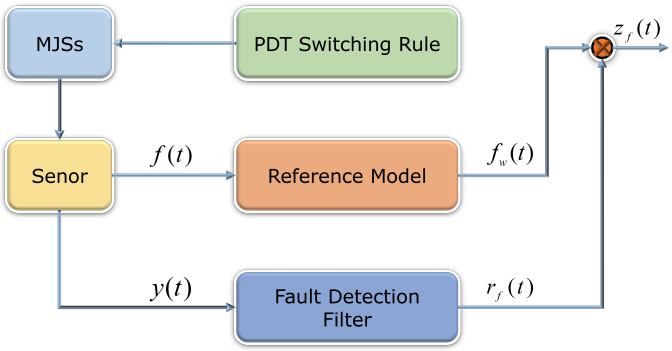


**Figure 1.** Framework of the FD filter for MJSs with PDT.

**Remark 1.** *In this paper, the PDT switching rule, which accurately describes the slow and fast intermittent switching, is used to describe the change of transition probabilities. This rule becomes more versatile as it can be simplified to the dwell-time or average dwell-time switching rule through the parameter settings. Furthermore, MJSs with PDT switching transition probabilities can also be reduced to traditional MJSs. Therefore, the switching model adopted in this paper is considered to be more comprehensive and universal.*

### 2.1. Model description

Consider the MJSs with time-varying delays and PDT as follows:

$$\begin{cases} \dot{x}(t) = A(\eta_t)x(t) + A_\varrho(\eta_t)x(t-\varrho(t)) + B(\eta_t)\omega(t) + D(\eta_t)f(t), \\ y(t) = C(\eta_t)x(t), \end{cases} \tag{2.1}$$

where $x(t) \in \mathbb{R}^n$, $y(t)$, $\omega(t)$, and $f(t) \in \mathbb{R}^p$ represent the state vector, measurement output vector, and external interference input that belongs to $l_2[0,\infty)$, and fault vector, respectively; and $\varrho(t)$ is the time-varying delay satisfying $0 \le \varrho(t) \le \bar{\varrho}$ and $\dot{\varrho}(t) \le u \le 1$, where $\bar{\varrho}$ and $u$ are constants. The stochastic process $\{\eta_t, t \ge 0\}$ denotes a continuous time Markov process in $\mathbb{M} = \{1, 2, \cdots, m\}$ with the transition probability matrix $\Pi = [\pi_{ij}^{\zeta(t)}]$ fulfilling

$$Pr\{\eta_{t+\Delta t} = j | \eta_t = i\} = \begin{cases} \pi_{ij}^{\zeta(t)} + o(\Delta t), i = j, \\ 1 + \pi_{ij}^{\zeta(t)} + o(\Delta t), i \ne j, \end{cases}$$

where $\pi_{ii}^{\zeta(t)} = -\sum_{j=1,j\neq i}^{m} \pi_{ij}^{\zeta(t)}$, $\pi_{ij}^{\zeta(t)} \geq 0$. The piecewise function $\zeta(t)$, which satisfies the PDT switching rule, takes values from a set $\mathbb{N} = \{1, 2, \cdots, N\}$. This PDT switching signal $\zeta(t)$ dictates the choice of the transition probability matrix $\pi_{ij}^{\zeta(t)}$, thereby directly influencing the stochastic dynamics of the MJSs. The mode-dependent interconnection weight matrices $A(\eta_t)$, $A_\varrho(\eta_t)$, $B(\eta_t)$, $D(\eta_t)$, and $C(\eta_t)$ are denoted as $A_i$, $A_{\varrho i}$, $B_i$, $D_i$, and $C_i$ for $\eta_t = i \in \mathbb{M}$, respectively.

**Remark 2.** *In Figure 2, the entire working interval is segmented into multiple stages according to the PDT switching rule. For any stage, it contains a certain subsystem running period (i.e., $\tau$-portion) and a persistence period (i.e., $T$-portion). Further, the duration of each $\tau$-portion is not less than $\tau_D$ and the duration of each $T$-portion is not more than $T_D$. For any active pth stage $[t_{s_p}, t_{s_{p+1}})$, $p \in \mathbb{N}$, all switching instants are expressed as $t_{s_p}, t_{s_p+1}, t_{s_p+2}, ..., t_{s_{p+1}}$, respectively. The interval $[t_{s_p}, t_{s_{p+1}})$ is partitioned into two sub-intervals $[t_{s_p}, t_{s_{p+1}}) \cup [t_{s_{p+1}}, t_{s_{p+1}})$. When $t \in [t_{s_p}, t_{s_{p+1}})$, just one certain subsystem is activated during the running time $\tau_A \geq \tau_D$. When $t \in [t_{s_{p+1}}, t_{s_{p+1}})$, any switching between subsystems can occur and the total running time $T_B$ satisfies $T_B \leq T_D$.*

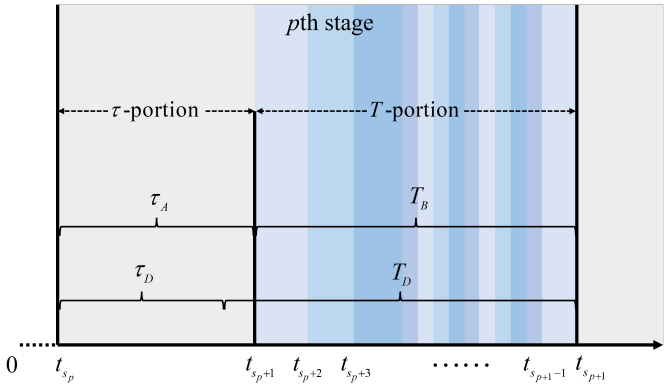


**Figure 2.** An illustration of the PDT switching rule.

### 2.2. Fault detection filter design

In order to realize the FD of MJS (2.1), this paper introduces a filter expressed as:

$$\begin{cases} \dot{x}_f(t) = A_{fi}x_f(t) + B_{fi}y(t), \\ r_f(t) = C_{fi}x_f(t), \end{cases} \tag{2.2}$$

where $x_f(t) \in \mathbb{R}^n$ and $y(t) \in \mathbb{R}^p$ denote the filter state vector and input signal filter, respectively; and $r_f(t)$ represents the residual signal compatible with the fault dimension. The matrices $A_{fi}$, $B_{fi}$, and $C_{fi}$ are filter gains to be determined later.

Incorporating the following fault weighting model can improve the FD capability:

$$\begin{cases} \dot{x}_w(t) = K_{w1}x_w(t) + K_{w2}f(t), \\ f_w(t) = K_{w3}x_w(t) + K_{w4}f(t), \end{cases} \tag{2.3}$$

where $x_w(t) \in \mathbb{R}^p$ and matrices $K_{w1}$, $K_{w2}$, $K_{w3}$, and $K_{w4}$ are given.

Let

$$\tilde{x}(t) = \left[x^T(t),\ x_f^T(t),\ x_w^T(t)\right]^T,\ \ \tilde{z}_e(t) = r_f(t) - f_w(t),\ \text{ and }\ v(t) = \left[\omega^T(t),\ f^T(t)\right]^T.$$

Based on (2.1)–(2.3), the residual system can be summarized below:

$$\begin{cases} \dot{\tilde{x}}(t) = \tilde{\mathcal{A}}\tilde{x}(t) + \tilde{\mathcal{B}}\tilde{x}(t - \varrho(t)) + \tilde{\mathcal{M}}v(t), \\ \tilde{z}_e(t) = \tilde{\mathcal{N}}_1\tilde{x}(t) + \tilde{\mathcal{N}}_2 v(t), \end{cases} \tag{2.4}$$

where

$$\tilde{\mathcal{A}} = \begin{bmatrix} A_i & 0 & 0 \\ B_{fi}C_i & A_{fi} & 0 \\ 0 & 0 & K_{w1} \end{bmatrix},\ \tilde{\mathcal{B}} = \begin{bmatrix} A_{\varrho i} & 0 & 0 \\ 0 & 0 & 0 \\ 0 & 0 & 0 \end{bmatrix},$$

$$\tilde{\mathcal{M}} = \begin{bmatrix} B_i & D_i \\ 0 & 0 \\ 0 & K_{w2} \end{bmatrix}, \tilde{\mathcal{N}}_1 = \left[0, C_{fi}, -K_{w3}\right],$$

$$\tilde{\mathcal{N}}_2 = [0, -K_{w4}].$$

### 2.3. Problem formulation

The objective of this paper is to design a FD method for the MJS (2.1) with time delays and PDT, where

(1) the residual system (2.4) with $v(t) = 0$ is globally uniformly exponentially stable (GUES);
(2) for $v(t) \neq 0$ and $\gamma > 0$, the following condition can be derived under zero initial conditions:

$$\int_{t=0}^{\infty} \tilde{z}_e^T(t)\tilde{z}_e(t)dt \leq \gamma^2 \int_{t=0}^{\infty} v^T(t)v(t)dt.$$

Additionally, to determine whether a fault has existed, we formulate the following residual evaluation function and threshold:

$$\mathcal{J}(r) \triangleq \int_{t_2}^{t_1} r_f^T(s)\, r_f(s)ds, \mathcal{J}_{th} \triangleq \sup_{f(t)=0} \mathcal{J}(r),$$

where $t_1$ and $t_2$ represent the initial and final evaluation moment, respectively. Then the following judgement logic can detected the fault signal:

$$\begin{cases} \mathcal{J}(r) > \mathcal{J}_{th} \Rightarrow \text{fault existed} \Rightarrow \text{alarm}, \\ \mathcal{J}(r) \leq \mathcal{J}_{th} \Rightarrow \text{with no fault}. \end{cases} \tag{2.5}$$

### 2.4. Preliminary

Before further discussion, several lemmas are necessary to facilitate the derivation of the results.

**Lemma 1** ([22]). *For a differential equation $V_i(t)$ on the interval $\Omega = (a, b)$ ($\Omega = [a, b)$ or $\Omega = (a, b]$), if there exist any time-varying functions $\psi(t)$ and $\phi(t)$ such that $\mathcal{L}V_i(t) \leq \psi(t)V_i(t) + \phi(t)$, then it can be derived that*

$$V_i(t) \leq V_i(a)e^{\Psi(t)} + \int_a^t e^{\Psi(t)-\Psi(r)}\phi(r)dr,$$

*for $t < b$, $\Psi(t) = \int_a^t \psi(r)dr$.*

**Lemma 2** ( [23]). *During the T-portion, the switching times $\Lambda(t_{s_p+1}, t_{s_{p+1}})$ are finite, indicating that Zeno behavior cannot occur. Hence, for any interval $[t_a, t_b)$ whose length is not less than $\tau_D + T_D$, the following inequality holds:*

$$0 \leq \Lambda(t_a, t_b) \leq \left(\frac{t_a - t_b}{T_D + \tau_D} + 1\right)(T_D f + 1),$$

*where $1/f$ denotes the minimum average switching interval in the T-portion.*

**Lemma 3** ([24]). *Given a symmetric matrix $R > 0$ and a differentiable function $\chi$ that varies over the interval $[\beta_1, \beta_2] \to \mathbb{R}^n$, it holds that:*

$$\int_{\beta_1}^{\beta_2} \dot{\chi}^T(s) R \dot{\chi}(s) ds \geq \frac{1}{\beta_2 - \beta_1} H_1^T R H_1 + \frac{3}{\beta_2 - \beta_1} H_2^T R H_2,$$

*where*

$$H_1 = \chi(\beta_2) - \chi(\beta_1), \quad H_2 = \chi(\beta_2) + \chi(\beta_1) - \frac{2}{\beta_2 - \beta_1} \int_{\beta_1}^{\beta_2} \chi(s) ds.$$

**Lemma 4** ( [25, 26]). *For a positive real number $0 < \alpha < 1$, any matrix N, and symmetric matrices $T_1 > 0$, $T_2 > 0$, it holds that:*

$$\begin{bmatrix} \frac{1}{\alpha} T_1 & 0 \\ 0 & \frac{1}{1-\alpha} T_2 \end{bmatrix} \geq \begin{bmatrix} T_1 + (1-\alpha)\left(T_1 - N T_2^{-1} N^T\right) & N \\ * & T_2 + \alpha\left(T_2 - N^T T_1^{-1} N\right) \end{bmatrix}.$$

## 3. Fault detection filter design

In this section, utilizing the L-K functional method, the FD problem of MJS (2.1) with PDT is investigated. For simplification, we define the following vectors and symbols:

$$\xi(t) = \left[x^T(t),\ x_f^T(t),\ x^T(t - \varrho(t)),\ x^T(t - \bar{\varrho}),\ v_1^T(t),\ v_2^T(t),\ x_w^T(t),\ f^T(t),\ w^T(t)\right]^T,$$
$$e_i = \left[0_{n\times(i-1)n}, I_n, 0_{n\times(6-i)n+3p}\right](i = 1, 2, \cdots, 6), v_1(t) = \int_{t-\varrho(t)}^{t} \frac{x(s)}{\varrho(t)} ds,$$
$$e_{i+6} = \left[0_{p\times 6n}, 0_{p\times(i-1)n}, I_p, 0_{p\times(3-i)p}\right](i = 1, 2, 3), v_2(t) = \int_{t-\bar{\varrho}}^{t-\varrho(t)} \frac{x(s)}{\varrho(t)} ds.$$

**Theorem 1.** *For given scalars $T_D$, $f$, $\alpha \in (0, 1)$, $\mu \in (1, \infty)$, $u$, and $\bar{\varrho}$, if there exist any matrices $G_i \in \mathbb{R}^n$, $X \in \mathbb{R}^{2n}$ and positive-definite matrices $P_i, Z_i, Q_1, Q_2, R \in \mathbb{R}^n$, $W_i \in \mathbb{R}^p$, such that the following conditions hold $\forall i, j \in \mathbb{M}$:*

$$\begin{bmatrix} \Xi|_{\varrho(t)=0} & E_1^T X \\ * & -e^{\alpha\bar{\varrho}} \tilde{R} \end{bmatrix} < 0, \tag{3.1}$$

$$\begin{bmatrix} \Xi|_{\varrho(t)=\bar{\varrho}} & E_2^T X^T \\ * & -e^{\alpha\bar{\varrho}} \tilde{R} \end{bmatrix} < 0, \tag{3.2}$$

$$\theta_j \leq \mu\theta_i, \tag{3.3}$$

$$T_D > \tau_D > max\left\{\frac{T_D f + 1}{\alpha}\ln\mu - T_D, \frac{1}{f}\right\}, \tag{3.4}$$

*where*

$$\begin{aligned}
\Xi &= \Phi_1 + \Phi_2 + \Phi_3 + \alpha\Pi_1^T\theta_i\Pi_1 + \Pi_3^T\Pi_3 - \gamma^2\Pi_4^T\Pi_4,\\
\Phi_1 &= \mathrm{Sym}\left\{\Pi_1^T\theta_i\Pi_2\right\} + \sum_{j\in\mathbb{M}}\pi_{ij}^{\zeta(t)}(\Pi_1^T\theta_j\Pi_1),\\
\Phi_2 &= e_1^T(Q_1+Q_2)e_1 - (1-u)e^{-\alpha\bar{\varrho}}e_3^TQ_1e_3 - e^{-\alpha\bar{\varrho}}e_4^TQ_2e_4,\\
\Phi_3 &= \bar{\varrho}^2\ell_1^TR\ell_1 - e^{-\alpha\bar{\varrho}}E_{12}^TR_rE_{12},\\
\Pi_1 &= \left[e_1^T,\ e_2^T,\ e_7^T\right]^T,\ \ \Pi_2 = \left[\ell_1^T,\ell_2^T,\ell_3^T\right]^T,\\
\Pi_3 &= C_{fi}e_2 - K_{w3}e_7 - K_{w4}e_8,\ \Pi_4 = \left[e_9^T,e_8^T\right]^T,\\
\ell_1 &= A_ie_1 + A_{\varrho i}e_3 + B_ie_8 + D_ie_9, \ell_2 = A_{fi}e_2 + B_{fi}C_ie_1, \ell_3 = K_{w1}e_7 + K_{w2}e_8,\\
E_1 &= \begin{bmatrix} e_1 - e_3 \\ e_1 + e_3 - 2e_5 \end{bmatrix},\ E_2 = \begin{bmatrix} e_3 - e_4 \\ e_3 + e_4 - 2e_6 \end{bmatrix},\\
E_{12} &= \left[E_1^T, E_2^T\right]^T, R_r = \begin{bmatrix} \frac{2\bar{\varrho}-\varrho(t)}{\bar{\varrho}}\tilde{R} & X \\ * & \frac{\bar{\varrho}+\varrho(t)}{\bar{\varrho}}\tilde{R} \end{bmatrix},\\
\tilde{R} &= \begin{bmatrix} R & 0 \\ 0 & 3R \end{bmatrix},\ \theta_i = \begin{bmatrix} P_i & G_i & 0 \\ G_i^T & Z_i & 0 \\ 0 & 0 & W_i \end{bmatrix},
\end{aligned}$$

*then the residual system (2.4) is GUES in $v(t) = 0$, while meeting the $H_\infty$ performance index $\gamma$ under a zero initial condition.*

*Proof.* Construct the L-K functional as $V(t) = V_1(t) + V_2(t) + V_3(t)$, where

$$\begin{aligned}
V_1(t) =&\ \tilde{x}^T(t)\theta_i\tilde{x}(t),\\
V_2(t) =&\ \int_{t-\varrho(t)}^{t} e^{\alpha(s-t)}x^T(s)Q_1x(s)ds + \int_{t-\bar{\varrho}}^{t} e^{\alpha(s-t)}x^T(s)Q_2x(s)ds,\\
V_3(t) =&\ \bar{\varrho}\int_{-\bar{\varrho}}^{0}\int_{t+\theta}^{t} e^{\alpha(s-t)}\dot{x}^T(s)R\dot{x}(s)dsd\theta.
\end{aligned}$$

Define $\mathcal{L}$ as the weak infinitesimal operator of $x(t)$, and evaluate the functional along residual system (2.4). We obtain

$$\mathcal{L}V_1(t) = \mathrm{Sym}\left\{\tilde{x}^T(t)\theta_i\dot{\tilde{x}}(t)\right\} + \sum_{j\in\mathbb{M}}\pi_{ij}^{\zeta(t)} \times (\tilde{x}^T(t)\theta_j\tilde{x}(t)) = \xi^T(t)\Phi_1\xi(t), \tag{3.5}$$

$$\begin{aligned}
\mathcal{L}V_2(t) \leq&\ -\alpha V_2(t) + x^T(t)(Q_1+Q_2)x(t) - (1-u)e^{-\alpha\bar{\varrho}}x^T(t-\varrho(t))Q_1x(t-\varrho(t))\\
&\ - e^{-\alpha\bar{\varrho}}x^T(t-\bar{\varrho})Q_2x(t-\bar{\varrho})\\
=&\ -\alpha V_2(t) + \xi^T(t)\Phi_2\xi(t),
\end{aligned} \tag{3.6}$$

$$\mathcal{L}V_3(t) \leq -\alpha V_3(t) + \bar{\varrho}^2 \dot{x}^T(t) R \dot{x}(t) - \bar{\varrho} e^{-\alpha\bar{\varrho}} \int_{t-\bar{\varrho}}^{t} \dot{x}^T(s) R \dot{x}(s) ds. \tag{3.7}$$

By employing Lemmas 3 and 4, one has

$$\begin{aligned} & -\bar{\varrho} e^{-\alpha\bar{\varrho}} \int_{t-\bar{\varrho}}^{t} \dot{x}^T(s) R \dot{x}(s) ds \\ \leq & \frac{\bar{\varrho} - \varrho(t)}{\bar{\varrho}} e^{-\alpha\bar{\varrho}} \kappa_1^T X \tilde{R}^{-1} X^T \kappa_1 + \frac{\varrho(t)}{\bar{\varrho}} e^{-\alpha\bar{\varrho}} \kappa_2^T X^T \tilde{R}^{-1} X \kappa_2 \\ & - e^{-\alpha\bar{\varrho}} \begin{bmatrix} \kappa_1 \\ \kappa_2 \end{bmatrix}^T \begin{bmatrix} \frac{2\bar{\varrho} - \varrho(t)}{\bar{\varrho}} \tilde{R} & X \\ * & \frac{\bar{\varrho} + \varrho(t)}{\bar{\varrho}} \tilde{R} \end{bmatrix} \begin{bmatrix} \kappa_1 \\ \kappa_2 \end{bmatrix}, \end{aligned} \tag{3.8}$$

where

$$\kappa_1 = \begin{bmatrix} x(t) - x(t - \varrho(t)) \\ x(t) + x(t - \varrho(t)) - 2v_1(t) \end{bmatrix}, \kappa_2 = \begin{bmatrix} x(t - \varrho(t)) - x(t - \bar{\varrho}) \\ x(t - \varrho(t)) + x(t - \bar{\varrho}) - 2v_2(t) \end{bmatrix}.$$

Summing up (3.7) and (3.8), we have

$$\mathcal{L}V_3(t) \leq -\alpha V_3(t) + \xi^T(t) \tilde{\Phi}_3 \xi(t), \tag{3.9}$$

where

$$\tilde{\Phi}_3 = \Phi_3 + \frac{\bar{\varrho} - \varrho(t)}{\bar{\varrho}} e^{-\alpha\bar{\varrho}} E_1^T X \tilde{R}^{-1} X^T E_1 + \frac{\varrho(t)}{\bar{\varrho}} e^{-\alpha\bar{\varrho}} E_2^T X^T \tilde{R}^{-1} X E_2.$$

In consideration of the $H_\infty$ performance, we define $F(t) = \tilde{z}_e^T(t)\tilde{z}_e(t) - \gamma^2 v^T(t)v(t)$. By choosing the target function $J = \mathcal{L}V(t) + \alpha V(t) + F(t)$, we get

$$J \leq \xi^T(t)(\Phi_1 + \Phi_2 + \tilde{\Phi}_3 + \alpha\Pi_1^T \theta_p \Pi_1 + \Pi_3^T \Pi_3 - \gamma^2 \Pi_4^T \Pi_4)\xi(t) = \xi^T(t)\Phi\xi(t). \tag{3.10}$$

Considering that $\Phi$ is a linear function of $\varrho(t)$, we have the following derivation for $\forall(\varrho(t)) \in [0, \bar{\varrho}]$:

$$\begin{cases} \Phi|_{\varrho(t)=0} < 0, \\ \Phi|_{\varrho(t)=\bar{\varrho}} < 0, \end{cases} \Rightarrow \Phi < 0. \tag{3.11}$$

Then, inequalities (3.1) and (3.2) are equal to $\Phi < 0$ by using the Schur complement, which means

$$\mathcal{L}V(t) \leq -\alpha V(t) - F(t). \tag{3.12}$$

When $t \in [t_{s_{p+1}-1}, t_{s_{p+1}})$ in Figure 2, the following inequality can be derived from condition (3.12) and Lemma 1:

$$V(t) \leq e^{-\alpha\left(t - t_{s_{p+1}-1}\right)} V\left(t_{s_{p+1}-1}\right) - \int_{t_{s_{p+1}-1}}^{t} e^{-\alpha(t-s)} F(s) ds. \tag{3.13}$$

From (3.3), the inequality can be obtained at the switching instant $t_{s_{p+1}-1}$:

$$V\left(t_{s_{p+1}-1}\right) \leq \mu V\left(t_{s_{p+1}-1}^-\right). \tag{3.14}$$

Obviously, each switching instant also applies to the above formula. By alternating the formulas (3.13) and (3.14) constantly, we can derive the function to the initial time $t_0 = 0$:

$$\begin{aligned} V(t) \leq & \mu e^{-\alpha\left(t-t_{s_{p+1}-1}\right)} V\left(t^-_{s_{p+1}-1}\right) - \int_{t_{s_{p+1}-1}}^{t} e^{-\alpha(t-s)} F(s) ds \\ \leq & \cdots \\ \leq & \mu^{\Lambda(t_0,t)} e^{-\alpha(t-t_0)} V(t_0) - \mu^{\Lambda(t_0,t)} \int_{t_0}^{t} e^{-\alpha(t-s)} F(s) ds, \end{aligned}$$

where $\Lambda(t_0, t)$ is the cumulative number of all switches in $(t_0, t)$. When $v(t) = 0$, $F(t) = \tilde{z}_e^T(t)\tilde{z}_e(t) \geq 0$ can be yielded. For $t \in [t_{s_p}, t_{s_{p+1}})$, the inequality is obtained:

$$V(t) \leq \mu^{\Lambda(t_0,t)} e^{-\alpha(t-t_0)} V(t_0) = e^{-\alpha(t-t_0)+\Lambda(t_0,t)\ln\mu} V(t_0). \tag{3.15}$$

According to Lemma 2, we have

$$0 \leq \Lambda(t_0, t) \leq \left(\frac{t - t_0}{T_D + \tau_D} + 1\right)(T_D f + 1). \tag{3.16}$$

From (3.15) and (3.16), we can get

$$V(t) \leq e^{\alpha t_0 + \left(1 - \frac{t_0}{T_D+\tau_D}\right)(T_D f+1)\ln\mu} e^{\left(\frac{(T_D f+1)\ln\mu}{T_D+\tau_D} - \alpha\right)t} V(t_0). \tag{3.17}$$

Due to this fact, there exist $k_1 > 0$ and $k_2 > 0$ satisfying

$$\begin{aligned} \|Z(t)\|^2 &= \max\{\|\tilde{x}(t)\|^2, \left\|\dot{\tilde{x}}(t)\right\|^2, \|\tilde{x}(t - \bar{\varrho})\|^2\}, \\ k_1 &= \min_{i\in\mathbb{M}}\{\lambda_{\min}(\theta_i)\} + \frac{1}{a}\lambda_{\min}(Q) + \frac{\bar{\varrho}^2}{a}\lambda_{\min}(R), \\ k_2 &= \max_{i\in\mathbb{M}}\{\lambda_{\max}(\theta_i)\} + \frac{1}{a}\lambda_{\max}(Q) + \frac{\bar{\varrho}^2}{a}\lambda_{\max}(R), \end{aligned}$$

which means

$$k_1 \|Z(t)\|^2 \leq V(t), V(t_0) \leq k_2 \|Z(t_0)\|^2.$$

Then from (3.17), we can further get

$$k_1 \|Z(t)\|^2 \leq k_2 e^{\alpha t_0 + \left(1 - \frac{t_0}{T_D+\tau_D}\right)(T_D f+1)\ln\mu} e^{\left(\frac{(T_D f+1)\ln\mu}{T_D+\tau_D} - \alpha\right)t} \|Z(t_0)\|^2. \tag{3.18}$$

Then, according to the above inequality, one can directly derive that

$$\|Z(t)\| \leq \sqrt{\frac{k_2}{k_1}} e^{\frac{1}{2}\left(\alpha t_0 + \left(1 - \frac{t_0}{T_D+\tau_D}\right)(T_D f+1)\ln\mu\right)} e^{\frac{1}{2}\left(\frac{(T_D f+1)\ln\mu}{T_D+\tau_D} - \alpha\right)t} \|Z(t_0)\|. \tag{3.19}$$

Since $p$ is chosen arbitrarily, the inequality (3.19) can be derived for other stages as well. According to (3.4), we can conclude that $\frac{(T_D f+1)\ln\mu}{T_D+\tau_D} - \alpha \leq 0$. At the same time, the residual system (2.4) satisfies GUES in $v(t) = 0$.

According to $\Phi < 0$, we can get $\int_{t_0}^{\infty} (\mathcal{L}V(s) + \alpha V(s) + F(s))ds \leq 0$. It is clear that $V(t) > 0$. Under zero initial conditions, we can also get

$$\int_{t_0}^{\infty} r^T(s)r(s)ds \leq \gamma^2 \int_{t_0}^{\infty} v^T(s)v(s)ds. \tag{3.20}$$

This finishes the proof. □

**Remark 3.** *If a constant $\kappa_0 > 0$ and a function $\Gamma$ exist such that $\|\tilde{x}(t)\| \leq \Gamma(\|\tilde{x}(0)\|, t), \forall t \geq 0$, $\kappa_0 \geq \|\tilde{x}(0)\|$, then for the initial condition and every switching signal $\zeta(t)$, the residual system (2.4) is globally uniformly asymptotically stable. In this paper, the above inequality is changed to the following form with $\varsigma > 0$ and $\psi \in (0, 1)$:*

$$\|\tilde{x}(t)\| \leq \varsigma\psi^t \|\tilde{x}(0)\|, \forall t \geq 0.$$

*So GUES is the special case of the stability above.*

**Remark 4.** *By employing the L-K functional method, the analysis of stability and $H_\infty$ performance for the residual system, which includes both time-varying delays and PDT, is performed in Theorem 1. In contrast to existing literature, this paper considers a more comprehensive range of information from the system models. When both time delays and PDT are considered simultaneously, it becomes difficult to analyze the stability of the residual system and solve the performance index. In this paper, by combining the switched system theory and L-K functional method, the globally uniformly exponential stability is obtained. Moreover, the weighted model is employed to enhance the sensitivity of the residual signal to the fault signal.*

On the basis of Theorem 1, the following contents explain the method of obtaining the filter gains.

**Theorem 2.** *We can given scalars $T_D$, $f$, $\alpha \in (0, 1)$, $\mu \in (1, \infty)$, $u$, and $\bar{\varrho}$. The residual system (2.4) is GUES in an $H_\infty$ performance index $\gamma$ if there exist positive-definite matrices $P_i, P_{fi}, Q_1, Q_2, R \in \mathbb{R}^n$, $W_i \in \mathbb{R}^p$, and any matrices $\tilde{A}_{fi} \in \mathbb{R}^n$, $\tilde{B}_{fi} \in \mathbb{R}^{n\times p}$, $\tilde{C}_{fi} \in \mathbb{R}^{p\times n}$, $X \in \mathbb{R}^{2n}$, such that (3.3), (3.4), and the following conditions hold $\forall i, j \in \mathbb{M}$:*

$$\begin{bmatrix} \tilde{\Xi}|_{\varrho(t)=0} & \tilde{\Pi}_3^T & E_1^T X \\ * & -I & 0 \\ * & * & -e^{\alpha\bar{\varrho}}\tilde{R} \end{bmatrix} < 0, \tag{3.21}$$

$$\begin{bmatrix} \tilde{\Xi}|_{\varrho(t)=\bar{\varrho}} & \tilde{\Pi}_3^T & E_2^T X^T \\ * & -I & 0 \\ * & * & -e^{\alpha\bar{\varrho}}\tilde{R} \end{bmatrix} < 0, \tag{3.22}$$

*where*

$$\begin{aligned}
&\tilde{\Xi} = \tilde{\Phi}_1 + \Phi_2 + \Phi_3 + \alpha\Pi_1^T\hat{\theta}_i\Pi_1 - \gamma^2\Pi_4^T\Pi_4, \\
&\tilde{\Phi}_1 = \mathrm{Sym}\left\{\Pi_1^T\tilde{\theta}_i\tilde{\Pi}_2\right\} + \sum_{j\in\mathbb{M}} \pi_{ij}^{\zeta(t)}(\Pi_1^T\hat{\theta}_j\Pi_1), \tilde{\Pi}_2 = \left[\ell_1^T, \tilde{\ell}_2^T, \ell_3^T\right]^T, \\
&\tilde{\Pi}_3 = \tilde{C}_{fi}e_2 - K_{w2}e_7 - K_{w4}e_8, \tilde{\ell}_2 = \tilde{A}_{fi}e_2 + \tilde{B}_{fi}C_ie_1,
\end{aligned}$$

$$\tilde{\theta}_i = \begin{bmatrix} P_i & I & 0 \\ P_{fi}^T & I & 0 \\ 0 & 0 & W_i \end{bmatrix}, \hat{\theta}_i = \begin{bmatrix} P_i & P_{fi} & 0 \\ P_{fi}^T & P_{fi} & 0 \\ 0 & 0 & W_i \end{bmatrix},$$

*with the other terms in (3.1) and (3.2). By the following equations, the gains can be obtained as*

$$A_{fi} = \tilde{A}_{fi} P_{fi}^{-1}, \quad B_{fi} = \tilde{B}_{fi}, \quad C_{fi} = \tilde{C}_{fi} P_{fi}^{-1}. \tag{3.23}$$

*Proof.* Through operation, $\Phi < 0$ in Theorem 1 is equal to

$$\hat{\Phi} = \begin{bmatrix} \Phi_0 & \Pi_3^T \\ * & -I \end{bmatrix} < 0, \tag{3.24}$$

where $\Phi_0 = \Phi_1 + \Phi_2 + \tilde{\Phi}_3 + \alpha \Pi_1^T \theta_i \Pi_1 - \gamma^2 \Pi_4^T \Pi_4$. Defining $\Im = \text{diag}\left\{I_n, G_i Z_i^{-1}, I_{4n+4p}\right\}$ and performing congruence transformation on both sides of $\hat{\Phi}$ by $\Im$ and $\Im^T$, we have

$$\begin{aligned} &\tilde{A}_{fi} = G_i A_{fi} Z_i^{-1} G_i^T, \tilde{B}_{fi} = G_i B_{fi}, \tilde{C}_{fi} = G_i Z_i^{-1} C_{fi}, \\ &P_{fi} = G_i Z_i^{-1} G_i^T, \Im \hat{\Phi} \Im^T = \begin{bmatrix} \tilde{\Phi}_0 & \tilde{\Pi}_3^T \\ * & -I \end{bmatrix}, \\ &\tilde{\Phi}_0 = \tilde{\Phi}_1 + \Phi_2 + \tilde{\Phi}_3 + \alpha \Pi_1^T \hat{\theta}_i \Pi_1 - \gamma^2 \Pi_4^T \Pi_4. \end{aligned}$$

Through utilizing the Schur complement, linear matrix inequalities (LMIs) (3.21) and (3.22) are equivalent to (3.1) and (3.2), respectively. Finally, we can get the filter gains as

$$A_{fi} = \tilde{A}_{fi} P_{fi}^{-1}, B_{fi} = \tilde{B}_{fi}, C_{fi} = \tilde{C}_{fi} P_{fi}^{-1}. \tag{3.25}$$

□

## 4. Illustrative example

This section uses a virus mutation processing system [27] to assess the effectiveness. Consider MJS (2.1) with the mathematical model as:

$$\begin{aligned} &\dot{x}(t) = (M_k - \delta I + \zeta H) x(t) + B_k w(t) + D_k f(t), \\ &y(t) = C_k x(t), \end{aligned}$$

where $w(t)$, $y(t)$, and $f(t)$ are the same as described in (2.1); $x(t)$ represents two different virus genotypes; $k = 1, 2$ denotes a Markov process; $\delta$ and $\zeta$ represent the decay rate and mutation rate, respectively; and $H = [H_{mn}]$ is the system matrix, where $H_{mn} \in \{0, 1\}$ represents a genetic link between genotypes.

$$\begin{aligned} &M_1 = \begin{bmatrix} 0.05 & 0 \\ 0 & 0.25 \end{bmatrix}, M_2 = \begin{bmatrix} 0.06 & 0 \\ 0 & 0.26 \end{bmatrix}, H = \begin{bmatrix} 0 & 1 \\ 1 & 0 \end{bmatrix}, B_1 = \begin{bmatrix} 0.5 \\ 0.1 \end{bmatrix}, B_2 = \begin{bmatrix} 0.3 \\ 0.2 \end{bmatrix}, \\ &D_1 = D_2 = \begin{bmatrix} 0.8 & 0.8 \end{bmatrix}, C_1 = \begin{bmatrix} 1.0 & 0 \end{bmatrix}, C_2 = \begin{bmatrix} 1.0 & 0 \end{bmatrix}, \zeta = 0.001, \\ &\delta = 0.68, \alpha = 0.159, \mu = 1.8, T_D = 3.4, f = 0.1. \end{aligned}$$

We assume that the mathematical model of virus mutation treatment includes a time-varying delay. The other parameters are specified as

$$\Pi^1 = \begin{bmatrix} -1.2 & 1.2 \\ 0.5 & -0.5 \end{bmatrix}, \Pi^2 = \begin{bmatrix} -1.1 & 1.1 \\ 0.6 & -0.6 \end{bmatrix}, \Pi^3 = \begin{bmatrix} -1 & 1 \\ 0.7 & -0.7 \end{bmatrix}, \varrho(t) = 1.2(1 - \cos(t)),$$
$$\bar{\varrho} = 2.4,\ u = 1.2, A_{\varrho 1} = \begin{bmatrix} 0.2 & 0.1 \\ 0.1 & 0.2 \end{bmatrix}, A_{\varrho 2} = \begin{bmatrix} 0.2 & 0.3 \\ 0.1 & 0.1 \end{bmatrix}.$$

The fault weighted system parameters are selected as $K_{w1} = -0.4,\ K_{w2} = 2,\ K_{w3} = 0.4,\ K_{w4} = -1$. The fault signal of the virus mutation processing system is expressed as

$$\text{Case 1:} f(t) = \begin{cases} 3\sin(t),\ 15 \le t \le 30, \\ 0\ ,\ \text{otherwise.} \end{cases}$$
$$\text{Case 2:} f(t) = \begin{cases} 3 \times e^{-0.3(t-15)},\ 15 \le t, \\ 0\ ,\ \text{otherwise.} \end{cases}$$

Solving the LMIs (3.21) and (3.22) can compute the optimal $H_\infty$ performance index $\gamma_{\min} = 1.4960$. Then we select $\gamma = 1.6$ to calculate the gain matrix of the FD filter:

$$A_{f1} = \begin{bmatrix} -3.6083 & 5.3774 \\ -0.5162 & -0.8749 \end{bmatrix},\ B_{f1} = \begin{bmatrix} -0.0880 \\ -0.0221 \end{bmatrix},\ C_{f1} = \begin{bmatrix} 0.0820 & -1.9623 \end{bmatrix},$$
$$A_{f2} = \begin{bmatrix} -5.5113 & 10.6125 \\ -1.0023 & -1.5441 \end{bmatrix},\ B_{f2} = \begin{bmatrix} -0.1257 \\ -0.0368 \end{bmatrix},\ C_{f2} = \begin{bmatrix} -0.0178 & -2.2430 \end{bmatrix}.$$

Assuming $x(0) = [0, 0]^T$, Figure 3 illustrates the system's hybrid switching behavior, showing both the stochastic Markov jumping process $\eta_t$ and the possible PDT switching signal $\zeta(t)$ that governs the time-varying transition probabilities. Under this switching policy, Figure 4 shows that the state trajectory $x(t)$ of the MJS converges to a bounded region in the presence of external disturbances and potential faults. Figure 5 depicts the profiles of the weighted fault signal $f_w(t)$ for both Cases 1 and 2. Figure 6 demonstrates that the residual signal $r_f(t)$ maintains a minimal magnitude in the fault-free scenario but exhibits a pronounced and sustained deviation immediately following fault occurrence at $t = 15\ s$ for both Cases 1 and 2. Figure 7 further shows the evaluation function $\mathcal{J}(r)$ exceeding the threshold $\mathcal{J}_{th}$ at $t = 15.3\ s$, successfully detecting the fault with a 0.3 $s$ delay and validating the proposed detection scheme.

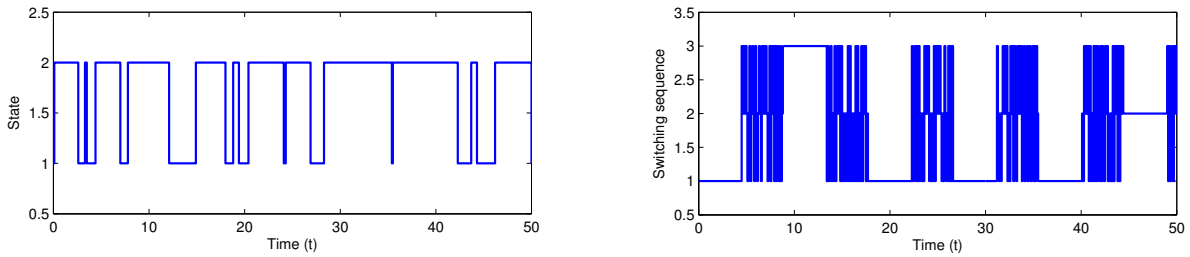


**Figure 3.** Random jumping mode of MJS (2.1) and the PDT switching sequence.

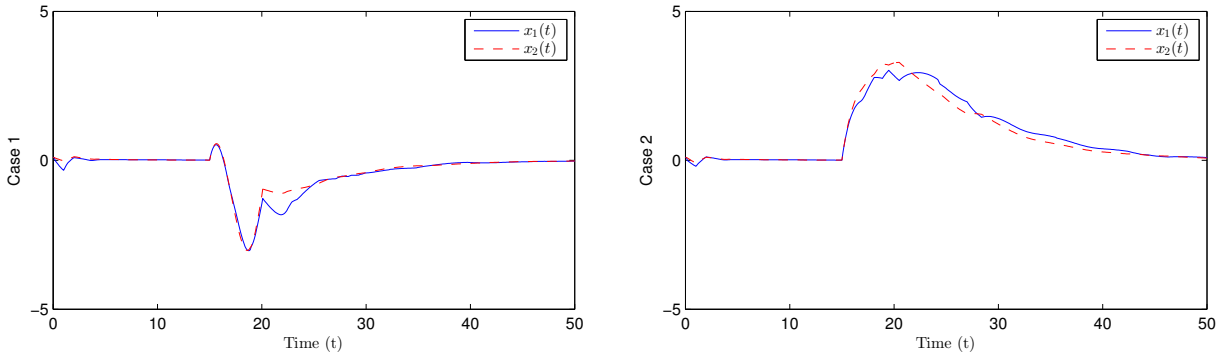


**Figure 4.** System response of MJS (2.1).

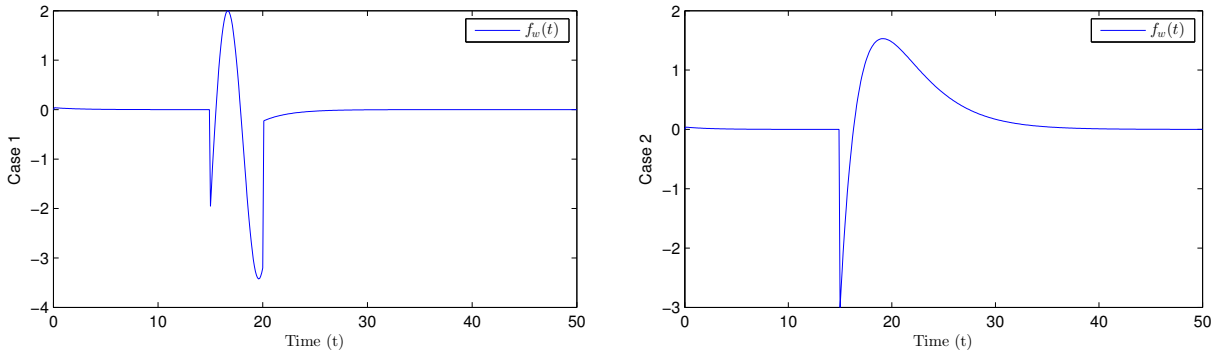


**Figure 5.** Weighted fault signal $f_w(t)$.

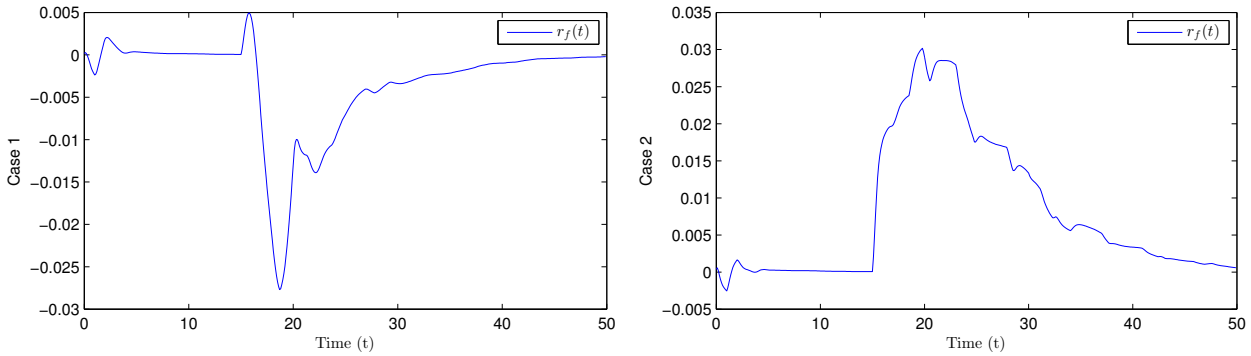


**Figure 6.** Residual response $r_f(t)$.

According to the residual evaluation mechanism, the threshold values $\mathcal{J}_{th}$ of the FD mechanism are calculated as $\mathcal{J}_{th} = 1.3312 \times 10^{-5}$ for Case 1 and $\mathcal{J}_{th} = 5.9303 \times 10^{-6}$ for Case 2, respectively. By analyzing the evaluation function values at multiple instants, we observe that $\int_0^{15.3} r_f^T(s) r_f(s) ds = 1.3840 \times 10^{-5} > \mathcal{J}_{th}$ in Case 1, and $\int_0^{15.3} r_f^T(s) r_f(s) ds = 7.2331 \times 10^{-6} > \mathcal{J}_{th}$ in Case 2. These results indicate that the fault occurring at $t = 15$ s is successfully detected by the designed filter after a short delay of 0.3 s in both scenarios. Therefore, the effectiveness of the proposed FD filter is validated

under different fault types.

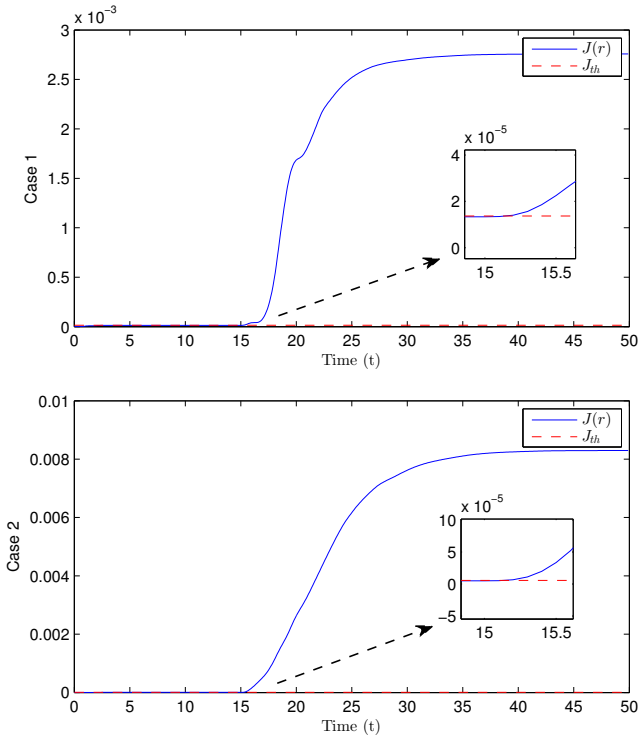


**Figure 7.** $\mathcal{J}_{th}$ and the evaluation function $\mathcal{J}(r)$.

## 5. Conclusions

In this article, the FD problem for the MJSs with time-varying delays and PDT has been addressed. The stochastic switching of the system mode was governed by a Markov chain, with its transition probabilities governed by the PDT switching rule. By the filter-based method, the FD problem has been reformulated as an $H_\infty$ filter design problem. By integrating the L-K functional method with switched system theory, the complexity arising from the coexistence of time delays and PDT was effectively addressed. By establishing LMIs and a PDT constraint condition, the filter was designed to guarantee GUES. Ultimately, a mathematical model of a viral mutation system was employed to validate the effectiveness.

## Author contributions

Zheng-Jin Zhang: Conceptualization, Writing—original draft, Software; Bin-Bin Gan: Methodology, Formal analysis, Writing—review and editing. All authors have read and approved the final version of the manuscript for publication.

## Use of Generative-AI tools declaration

The authors declare they have not used Artificial Intelligence (AI) tools in the creation of this article.

## Acknowledgments

This work was supported in part by the Taishan Scholar Special Project Fund (Grant No. TSQN202507165), and the Shandong Provincial Natural Science Foundation (Grant No. 2023HWYQ-086).

## Conflict of interest

The authors declare no conflicts of interest.

## References

1. J. Wang, D. Wang, H. Yan, H. Shen, Composite antidisturbance $\mathcal{H}_\infty$ control for hidden Markov jump systems with multi-sensor against replay attacks, *IEEE Trans. Autom. Control*, **69** (2023), 1760–1766. https://doi.org/10.1109/TAC.2023.3326861

2. J. Wang, J. Wu, H. Shen, J. Cao, L. Rutkowski, Fuzzy $H_\infty$ control of discrete-time nonlinear Markov jump systems via a novel hybrid reinforcement $Q$-learning method, *IEEE Trans. Cybern.*, **53** (2022), 7380–7391. https://doi.org/10.1109/TCYB.2022.3220537

3. W. Fan, J. Yan, S. Huang, W. Liu, Research and prediction of opioid crisis based on BP neural network and Markov chain, *AIMS Math.*, **4** (2019), 1357–1368. https://doi.org/10.3934/math.2019.5.1357

4. X. Mao, W. Shan, J. Yu, Automatic diagnosis and subtyping of ischemic stroke based on a multi-dimensional deep learning system, *IEEE Trans. Instrum. Meas.,* **73** (2024), 1–11. https://doi.org/10.1109/TIM.2024.3458059

5. H. Shen, F. Li, S. Xu, V. Sreeram, Slow state variables feedback stabilization for semi-Markov jump systems with singular perturbations, *IEEE Trans. Autom. Control*, **63** (2018), 2709–2714. https://doi.org/10.1109/TAC.2017.2774006

6. W. Lin, G. Tan, Q. Wang, J. Yu, Fault-tolerant state estimation for Markov jump neural networks with time-varying delays, *IEEE Trans. Circuits Syst. II*, **71** (2024), 2114–2118. https://doi.org/10.1109/TCSII.2023.3332390

7. G. Tan, W. Chen, J. Yang, X. Tran, Z. Li, Dual control for autonomous airborne source search with Nesterov accelerated gradient descent: algorithm and performance analysis, *Neurocomputing*, **630** (2025), 129729. https://doi.org/10.1016/j.neucom.2025.129729

8. C. Qin, W. Lin, J. Yu, Adaptive event-triggered fault detection for Markov jump nonlinear systems with time delays and uncertain parameters, *Int. J. Robust Nonlinear Control*, **34** (2024), 1939–1955. https://doi.org/10.1002/rnc.7062

9. G. Tan, T. Wang, A new result on $H_\infty$ filtering criterion based on improved techniques, *Circuits Syst. Signal Process.*, 2025, 1–18. https://doi.org/10.1007/s00034-025-03305-4

10. L. Zhang, Y. Sun, Y. Pan, H. K. Lam, Reduced-order fault detection filter design for fuzzy semi-Markov jump systems with partly unknown transition rates, *IEEE Trans. Syst. Man Cybern: Syst.*, **52** (2022), 7702–7713. https://doi.org/10.1109/TSMC.2022.3163719

11. H. Shen, W. J. Lin, Z. Lian, Sampled-data stabilization of Markovian jumping conic-type nonlinear systems via an augmented looped functional, *Commun. Nonlinear Sci. Numer. Simul.*, **147** (2025), 108814. https://doi.org/10.1016/j.cnsns.2025.108814

12. K. Yin, D. Yang, Asynchronous fault detection filter of positive Markov jump systems by dynamic event-triggered mechanism, *ISA Trans.*, **138** (2023), 197–211. https://doi.org/10.1016/j.isatra.2023.03.017

13. A. S. Morse, Supervisory control of families of linear set-point controllers-Part I. Exact matching, *IEEE Trans. Autom. Control*, **41** (1996), 1413–1431. https://doi.org/10.1109/9.539424

14. H. Geng, H. Zhang, A new $H_\infty$ control method of switched nonlinear systems with persistent dwell time: $H_\infty$ fuzzy control criterion with convergence rate constraints, *AIMS Math.*, **9** (2024), 26092–26113. https://doi.org/10.3934/math.20241275

15. S. Li, J. Lian, Almost sure stability of Markov jump systems with persistent dwell time switching, *IEEE Trans. Syst. Man Cybern. Syst.*, **51** (2020), 6681–6690. https://doi.org/10.1109/TSMC.2020.2964034

16. J. Wang, J. Wu, J. Cao, J. H. Park, H. Shen, $\mathcal{H}_\infty$ fuzzy dynamic output feedback reliable control for Markov jump nonlinear systems with PDT switched transition probabilities and its application, *IEEE Trans. Fuzzy Syst.*, **30** (2021), 3113–3124. https://doi.org/10.1109/TFUZZ.2021.3104336

17. W. Lin, Q. Han, X. Zhang, J. Yu, Reachable set synthesis of Markov jump systems with time-varying delays and mismatched modes, *IEEE Trans. Circuits Syst. II*, **69** (2021), 2186–2190. https://doi.org/10.1109/TCSII.2021.3126262

18. W. Lin, Q. Wang, G. Tan, Asynchronous adaptive event-triggered fault detection for delayed Markov jump neural networks: a delay-variation-dependent approach, *Neural Netw.*, **171** (2024), 53–60. https://doi.org/10.1016/j.neunet.2023.12.010

19. W. Liu, X. Fan, G. Tan, W. J. Lin, Reachable set control of cyber-physical systems with Markov jump parameters and hybrid attacks, *IEEE Trans. Autom. Sci. Eng.*, **22** (2025), 18673–18681. https://doi.org/10.1109/TASE.2025.3589031

20. S. Jia, W. J. Lin, Adaptive event-triggered reachable set control for Markov jump cyber-physical systems with time-varying delays, *AIMS Math.*, **9** (2024), 25127–25144. https://doi.org/10.3934/math.20241225

21. G. Zhong, G. Yang, Simultaneous control and fault detection for discrete-time switched delay systems under the improved persistent dwell time switching, *IET Control Theory Appl.*, **10** (2016), 814–824. https://doi.org/10.1049/iet-cta.2015.0925

22. G. Göksu, U. Başer, Observer-based H∞ finite-time control for switched linear systems with interval time-delay, *Trans. Inst. Meas. Control*, **41** (2019), 1348–1360. https://doi.org/10.1177/0142331218777559

23. H. Shen, Z. Huang, J. Cao, J. H. Park, Exponential $H_\infty$ filtering for continuous-time switched neural networks under persistent dwell-time switching regularity, *IEEE Trans. Cybern.*, **50** (2019), 2440–2449. https://doi.org/10.1109/TCYB.2019.2901867

24. A. Seuret, F. Gouaisbaut, Wirtinger-based integral inequality: application to time-delay systems, *Automatica*, **49** (2013), 2860–2866. https://doi.org/10.1016/j.automatica.2013.05.030

25. C. Zhang, Y. He, L. Jiang, M. Wu, Q. Wang, An extended reciprocally convex matrix inequality for stability analysis of systems with time-varying delay, *Automatica*, **85** (2017), 481–485. https://doi.org/10.1016/j.automatica.2017.07.056

26. X. Zhang, Q. Han, A. Seuret, F. Gouaisbaut, Y. He, Overview of recent advances in stability of linear systems with time-varying delays, *IET Control Theory Appl.*, **13** (2019), 1–16. https://doi.org/10.1049/iet-cta.2018.5188

27. W. Qi, J. H. Park, J. Cheng, Y. Kao, X. Gao, Exponential stability and $\mathcal{L}_1$-gain analysis for positive time-delay Markovian jump systems with switching transition rates subject to average dwell time, *Inf. Sci.*, **424** (2018), 224–234. https://doi.org/10.1016/j.ins.2017.10.008


AIMS Press

© 2025 the Author(s), licensee AIMS Press. This is an open access article distributed under the terms of the Creative Commons Attribution License (https://creativecommons.org/licenses/by/4.0)